CORE
Metadata, citation and similar papers at core.ac.uk
Provided by UNT Digital Library

LM-06K126
October 30, 2006

Analysis of Carrier Recombination Processes in 0.6 eV InGaAs Epitaxial Materials for Thermophotovoltaic Devices

D Donetsky, F Newman, M Dashiell

NOTICE

This report was prepared as an account of work sponsored by the United States Government. Neither the United States, nor the United States Department of Energy, nor any of their employees, nor any of their contractors, subcontractors, or their employees, makes any warranty, express or implied, or assumes any legal liability or responsibility for the accuracy, completeness or usefulness of any information, apparatus, product or process disclosed, or represents that its use would not infringe privately owned rights.

Analysis of carrier recombination processes in 0.6 eV InGaAs epitaxial materials for thermophotovoltaic devices

D. Donetsky, F. Newman, M. Dashiell

Department of ECE, Stony Brook University, NY 11794-2350
Emcore Photovoltaics, Inc., Albuquerque, NM 87123
Lockheed Martin Corp., Schenectady, NY 12301

Abstract

Minority carrier lifetime was measured by time-resolved photoluminescence (TRPL) method in sets of p-type and n-type InGaAs double heterostructures (DH) moderately doped with Zn and Te, respectively. Contributions of the radiative and non-radiative recombination terms were separated by fitting experimental data to temperature dependences of the radiative term. The latter was modeled with measured fundamental absorption spectrum and the temperature dependence of the photon recycling effect was taken into account. Different temperature dependences of radiative terms for electron and hole materials were obtained. It was concluded that in 0.6 eV Te-doped InGaAs structures the radiative recombination controls the hole lifetime at liquid nitrogen temperatures, while Auger recombination dominates at room and above room temperatures. In similar 0.6 eV InGaAs with Zn-doped active regions Shockley-Read-Hall (SRH) recombination was found dominant in a wide temperature range from liquid nitrogen to above–room temperatures. Rapid decrease of electron lifetime with decrease of excess carrier concentration was observed and attributed to recombination through partially-ionized deep donor centers. The obtained data allows for more adequate modeling of the performance and design optimization of narrow-gap photonic devices based on InGaAs Indium-rich compounds.

1. Introduction

Indium-rich InGaAs epitaxial materials grown with InPAs buffer layers lattice-mismatched to the InP substrates are being developed [1,2]. Minority carrier lifetime constants of several microseconds were demonstrated in DH with unintentionally doped ($n < 10^{15}$ cm^{-3}) 0.5-0.6 eV InGaAs active regions [3]. Due to large carrier lifetime the materials are favorable for photovoltaic applications including thermophotovoltaic (TPV) energy conversion [4]. TPV devices with energy conversion efficiency of 24 % have been demonstrated [5]. Further improvement of the TPV device performance requires better understanding the carrier recombination channels limiting the device open circuit voltage. This work summarizes the results of study of minority carrier lifetime in structures with different doping. The work was motivated with the need of an empirical model that will satisfactory predict change of the device performance with variation of design, primarily, doping and thickness of the active layer. In order to determine these parameters consistently, the minority carrier lifetime measurements were performed in sets of double heterostructures where only one parameter was varied at a time.

2. Analysis of radiative recombination in 0.6 eV InGaAs

In analysis of carrier recombination processes in bulk materials it is often assumed that temperature dependence of radiative lifetime is described asymptotically by T^{β} with β = 1.5 [6,7]. To observe such dependence experimentally two major conditions have to be met

(1) Fundamental absorption edge spectrum should be well approximated by function $A\sqrt{h\nu - \varepsilon_g}/h\nu$ in a whole range of spontaneous emission spectrum; in this case the $T^{1.5}$ asymptote will be valid for both non-degenerate and degenerate carrier statistics[1];

(2) Absorbing layer thickness should be small compared to the absorption length in order to neglect the effect of reabsorption (photon recycling).

In addition, the $T^{1.5}$ approximation does not take into account temperature dependence of energy gap and assumes large bandgap energy ε_g compared to thermal energy k_BT. In

[1] see appendix

most cases of interest condition $\varepsilon_g/k_BT >> 1$ is satisfied which enables a simple way for incorporation of the bandgap temperature dependence into the model[2].

In this paper it is shown that small deviations of energy absorption spectrum from the approximation in condition (1) result in essentially different dependences of radiative recombination on temperature for electron and hole materials. Temperature dependences of minority carrier lifetime for both electrons and holes were found to be slower than $T^{1.5}$. The role of self-absorption decreases with cooling due to narrowing of the spontaneous emission spectrum toward the absorption edge. Thus, temperature dependence of photon recycling makes the experimental dependence of carrier lifetime on temperature faster, especially in the cryogenic range. This dependence was calculated using the developed model and allowed for explanation of experimental data in the entire temperature range.

For analysis we used approach similar to one presented in [88]. Spontaneous emission rate Q (the number of photons per unity time) is the rate of decay of excess carrier concentration $\Delta n/\tau$, so that $Q = -\Delta n/\tau$. Spectral density of spontaneous emission rate, dq_{sp}, is defined by product of photon state density $\rho = 8\pi(N/c)^3v^2/h$ where N is the refractive index, electron and hole distribution functions f_c and f_v and matrix elements $|H^v_{cv}|^2$ for direct transitions from conduction to valence bands.

$$dq_{sp} = \frac{2\pi}{\hbar}\sum_k \left|H^v_{cv}\right|^2 \delta\left[\varepsilon_c(k) - \varepsilon_v(k) - hv\right] f_c^e\, f_v^h\, \rho dv \qquad (1)$$

The same matrix elements define fundamental absorption spectrum $\alpha(hv)$

$$\alpha(hv) = \left(\frac{N}{c}\right)\frac{2\pi}{\hbar}\sum_k \left|H^v_{cv}\right|^2 \delta\left[\varepsilon_c(k) - \varepsilon_v(k) - hv\right](1 - f_v^h - f_c^e)dv \qquad (2)$$

Since the latter can be determined experimentally, the rate of spontaneous emission is often expressed in terms of the experimental absorption spectrum. The absorption

[2] see appendix

spectrum is typically measured in an undoped material where band filling effects are negligible due to f_c, $f_v << 1$

$$dq_{sp} = \frac{\alpha(h\nu)}{1 - f_v^h - f_c^e} \frac{c}{N} f_c^e f_v^h \rho d\nu \approx \alpha(h\nu) \frac{c}{N} f_c^e f_v^h \rho d\nu . \quad (3)$$

In the case of general carrier distribution functions with quasi-Fermi levels F_e and F_h one has

$$dq_{sp} = \frac{8\pi N^2}{h^3 c^2} \frac{\alpha(h\nu) \cdot (h\nu)^2}{\left(\exp\left(\frac{\varepsilon_c(\nu) - F_e}{k_B T} \right) + 1 \right) \left(\exp\left(\frac{\varepsilon_v(\nu) - F_h}{k_B T} \right) + 1 \right)} d(h\nu) . \quad (4)$$

Here ε_c and ε_v are electron and hole energies in conduction and valence bands corresponding to direct optical transitions with photon energy $h\nu$ (see inset in Figure 1). Introducing reduced effective mass $m_{cv} = (m_c^{-1} + m_v^{-1})^{-1}$ and using substitution $\Delta\varepsilon = h\nu - \varepsilon_g = \varepsilon_c + \varepsilon_v$ one can express ε_c and ε_v as function of excess of photon energy above the bandgap energy $\Delta\varepsilon$

$$\varepsilon_c = \frac{\hbar^2 k^2}{2m_e} = \Delta\varepsilon \frac{m_{cv}}{m_c} \qquad \varepsilon_v = \frac{\hbar^2 k^2}{2m_e} = \Delta\varepsilon \frac{m_{cv}}{m_v} \quad (5)$$

The total recombination rate was obtained by integration of the spectral density over the entire spectrum of spontaneous emission from 0.585 to 0.9 eV (Figure 2).

$$Q_{sp} = \frac{8\pi N^2}{h^3 c^2} \int_{0.585eV}^{0.9eV} \frac{\alpha(h\nu) \cdot (h\nu)^2}{\left(\exp\left(\frac{(h\nu - \varepsilon_g) m_{cv}/m_c - F_e}{k_B T} \right) + 1 \right) \left(\exp\left(\frac{(h\nu - \varepsilon_g) m_{cv}/m_v - F_h}{k_B T} \right) + 1 \right)} d(h\nu) \quad (6)$$

The refractive index was calculated as $N = 3.4$. For numerical integration the experimental absorption spectrum was split into three intervals: namely, 0.585 - 0.605 eV

for the absorption tail with positive curvature, 0.605 - 0.64 eV for the absorption edge with negative curvature, and 0.64 - 0.9 eV for a non-parabolic part of the spectrum with positive curvature. Each of the pieces was approximated by a polynomial function of the 5^{th} order. The polynomial fits presented in Figure 2 matches the experimental spectrum exactly so that the difference is hardly seen. An alternative square-root fitting is shown in Figure 2 as well. One can see that the square-root fitting with only one parameter *A* does not describe the absorption spectrum adequately.

Finally, minority carrier lifetime τ was calculated as excess carrier concentration Δn over the recombination rate, $\tau = \Delta n/Q_{sp}$, where the excess carrier concentration was obtained as a product of the density of states and integral Fermi

$$\Delta n = \left(\frac{m_e k_B T}{\hbar^2}\right)^{3/2} \cdot \frac{2^{1/2}}{\pi^2} \int_{\Delta\varepsilon=0}^{\infty} \frac{\sqrt{\Delta\varepsilon}\, d\Delta\varepsilon}{\exp(\Delta\varepsilon - F_e/k_B T)+1} \qquad (7)$$

Temperature dependences of the quasi-Fermi levels for majority carrier concentrations were obtained with approximation of the integral Fermi [9] valid in entire range of the argument with better than 1% accuracy. The effective masses for electrons and hole were calculated as m_e = 0.046 and m_h = 0.478 resulting in densities of states of $N_c = 2.5 \cdot 10^{17}$ and $N_v = 8.3 \cdot 10^{18}$ cm^{-3}, respectively. For illustrative purposes these dependences are shown in Figure 1 calculated for several electron and hole concentrations within the ranges of sample doping. One can see that the hole distribution functions remain non-degenerate in the entire ranges of temperatures and doping, while electron distribution functions are weakly degenerate except the case of DH with the smallest carrier concentration at room temperatures.

The results of integration of the absorption spectrum in accordance with expression (6) are presented in Figure 3. In the case of non-degenerate carrier statistics with background carrier concentrations of 1 x 10^{16} cm^{-3} temperature dependences of minority carrier lifetime were found to be essentially the same for both electron and hole materials in a whole temperature range. As background concentration increases, the difference between electron and hole lifetimes increases primarily in low temperatures. One can see that in the T^{β} approximation parameter β changes with temperature for a

given carrier concentration and slightly increases with carrier concentration. The latter increase is small for electron lifetimes and considerable for hole lifetimes. For comparison with experimental data, parameter β was extracted in the temperature range from 80 to 200 K for p-type and n-type materials with the same carrier concentration of 1 x 10^{17} cm^{-3}. In the specified range it was found to be β=0.64 and β=1.0 for hole and electron materials, respectively. Note, that values of β-parameter are significantly lower than asymptotical value of 1.5 and lower than that obtained with use of the alternative square-root spectrum fit (Figure 2)[3]. The room-temperature value of radiative recombination coefficient B was calculated to be ≈2 x 10^{-10} cm^3/s for both electrons and holes.

In structures with thick absorption layers the experimental values of radiative lifetime were expected to be longer due to the effect of self-absorption. The enhancement of radiative lifetime due to this effect was characterized by photon recycling coefficient $\phi = \tau_{rad\_exp}/\tau_{rad\_theor}$ [10,11]. Figure 2 illustrates that the absorption and spontaneous emission spectra at room temperature overlap essentially. As temperature decreases, the spontaneous emission spectrum becomes narrower toward the absorption edge, the average absorption coefficient becomes smaller and recycling coefficient decreases. The expression for recycling coefficient was obtained using the approach similar to one presented in [12]. In addition to that work our calculations (see equations below) take into account multiple photon reflections from the front and back interfaces of the active region (inset to Figure 4). Details on the derivation of the analytical expression will be published elsewhere [13].

$$\phi(W) = \frac{1}{1 - \frac{1}{d}\int_0^W F(z)dz} \tag{8}$$

where

$$F(z) = \int_{hv=Eg}^{\infty} \int_{z'=0}^{z'=W} I_{Sp}(hv)\alpha(hv)\frac{1}{2}\{E_i(\alpha|z-z'| + R_1(\theta' < \theta'_{cr})E_i(\alpha|z-z'|) +$$

[3] see appendix

$$+\left[1-R_1(\theta'<\theta'_{cr})\right]E_i\left(\frac{\alpha|z-z'|}{\cos(\theta''_{cr})}\right)+E_i\left(\frac{\alpha|2d-z-z'|}{\cos(\theta''_{cr})}\right)d(h\nu)dz' \quad (9)$$

Here I_{sp} is the normalized spectrum of spontaneous emission, $\alpha(h\nu)$ is absorption coefficient, W is the active layer thickness, R_1 and R_2 are reflection coefficients for the front and back surfaces, E_i is exponential integral function defined as

$$E_i(x)=\int_x^{\infty}\frac{\exp(-x)}{x}dx \quad (10)$$

As expected, figure 4 shows the temperature dependence of the photon recycling coefficient was found to be strong, in the range from T = 80 to 200 K it increments β in T^{β} with additional $\Delta\beta = 0.53$. Temperature dependence of the bandgap also contributes to the lifetime temperature dependence, although in a lesser extent. The increment $\Delta\beta$ = 0.048 from the bandgap change with temperature was added into the model[2].

Thus, analysis showed that in epitaxial 0.6 eV InGaAs temperature dependence of minority carrier lifetime should the expected slower than $T^{1.5}$ for electrons and considerably slower than that for holes.

3. Structures

The double heterostructures (DH) were grown on InP substrates by OMVPE. The 0.6 eV InGaAs active layers were 2 μm thick. The excess carriers were confined with lattice-matched InPAs windows with the thickness of 50 nm. Lattice-mismatching of the InGaAs layer and InP substrate was accommodated with three step-graded InPAs buffer layers. The InPAs layers were grown lattice-matched to InGaAs to avoid carrier recombination at the interfaces. The energy gap of the InPAs carrier confinement layers of 1.0 eV was large enough to prevent leakage of non-equilibrium carriers over the barriers. The doping concentration in the active region was varied to obtain free carrier concentration in the range from 1 x 10^{16} to 3 x 10^{17} for the p-type layers and from 8.5 x 10^{16} to 5 x 10^{17} for the n-type layers. The window layer doping was of the same type as

doping of the active region for adequate carrier confinement. Details of the growth procedure can be found elsewhere [14,15].

4. Experimental approach

Minority carrier lifetime was measured by direct method, the time-resolved photoluminescence (TRPL) technique. Schematic diagram of the setup is shown in Figure 5. The excess carriers were excited either by 532-nm or 1,064 nm Q-switched Nd:YAG lasers both with a 0.5 ns pulse width and repetition rate of 6.6 kHz. The photoluminescence (PL) was collected with reflective optics and focused on a small-area photodiode with a decay time constant of 1 ns. The PL decays were sampled by a digital scope with the acquisition rate of 5 GS/s and averaged. The averaging was needed to obtain PL dynamic ranges of at least two-orders of magnitude in order to verify that decays are of exponential form and to preserve accuracy in determination of lifetime constants. Details of the setup were described earlier [16].

5. Experimental results and discussion

5.1. Hole lifetime in Tellurium-doped 0.6-eV InGaAs

Typical PL decays observed in DHs with n-type active regions are shown in Figure 6. The PL decays in all n-InGaAs structures were found to be of exponential form with a single time constant independent on excess carrier concentration. The lifetime constants were determined in the ranges of excess carrier concentration well below the background doping level. Temperature dependences of the PL decay constants are shown in Figure 7. One can see that the time constants decrease rapidly with cooling. The dashed lines represent fittings made with the radiative recombination terms obtained with the analysis described above. Temperature dependences of both the photon recycling coefficient and energy bandgap were taken into account. A free carrier concentration was the only parameter of fitting. The inset shows the non-radiative recombination term obtained as a function of free carrier concentration at the room temperature. This term fits satisfactory with square dependence on free carrier concentration which allows associating it with Auger recombination. Indeed, it was shown by calculations that in electron materials with

weak degeneration the Auger recombination term still remains to be dependent as a square of free carrier concentration and deviation toward a linear dependence on doping appears to be under stronger degeneration [17]. Thus, the non-radiative lifetime at room temperature is characterized by Auger coefficient of C_n = 3.2 x 10^{-28} cm^6/s. The value of this coefficient matches well to values reported previously for the InGaAs lattice-matched to InP [18] and for undoped 0.6-eV InGaAs [6] similar to the materials studied in this work. We assumed that the observed strong Auger recombination in 0.6-eV InGaAs originates from direct CHCC process rather than phonon-assistant process [17]. For the CHCC process it was shown that order of magnitude of Auger coefficient can be estimated as follows [19]

$$C_n \sim \left(\frac{m_c}{m_v}\right)^{3/2} \frac{\hbar^3}{m_c^2\sqrt{E_g \cdot k_B T}} \left(\frac{e^2}{\varepsilon E_g}\right)^2 \exp\left(-\frac{\varepsilon_{th}}{k_B T}\right), \tag{11}$$

where ε is the dielectric function, $\varepsilon_{th} \sim m_c/m_v E_g$ is the threshold or activation energy for Auger process. The value of C_n estimated with expression (11) matches the order of magnitude for the experimental value which supports the assumption about the origin of Auger recombination. This expression was used to fit the experimental data and to determine the threshold energy for the CHCC Auger process (Figure 8). The threshold energy was found to be 40 meV which is lower than the value obtained theoretically. Also authors of [16] noted that the experimental value of activation energy is expected to be lower than the value obtained in their analysis due to neglected warping of isoenergetic surfaces in the valence bands. The experimental activation energy correlates with experimental data of 33 meV reported in [6] and 40 meV reported in [20]. It should be noted, however, that authors of both papers studied undoped materials and interpreted non-radiative transitions with the CHSH process. In this case the extracted threshold energies were associated with distance between bandgap energy E_g and spin-orbit splitting Δ_{so}. In the present work the Auger processes were observed in a set of n-doped structures which excludes interpretation of the effect with the CHSH transitions.

Thus, Auger recombination was found dominating at room temperature in n-type 0.6 eV InGaAs epitaxial materials doped in the range of (0.8-5) x 10^{17} cm^{-3}.

Measurements of hole lifetime in the set of n-type DH with different doping verified the radiative recombination model used for analysis of temperature dependence of electron lifetime in p-type material.

5.2. Electron lifetime in Zinc-doped 0.6-eV InGaAs

The Zn-doped DHs were measured under the same experimental conditions. Typical PL decays are shown in Figure 9a for several excitation levels and in Figure 9b for several samples with different acceptor concentration in the active region. Concentrations of photoexcited carriers at PL maxima were kept below the background free carrier concentration. All the PL decays in p-type structures showed non-exponential recombination kinetics with decrease of instantaneous carrier lifetime along the PL decay. At any fixed PL intensity level (or excess carrier concentration) the instantaneous lifetime was similar for all PL decays with different initial excess carrier concentrations (Figure 9a). Thus, one can conclude that the instantaneous lifetime is a function of excess carrier concentration. The intensity-dependent carrier lifetime indicated strong contribution of Shockley-Read–Hall (SRH) recombination to the overall carrier lifetime. Note that the rapid decrease of the instantaneous lifetime along the PL decays progresses with doping (Figure 9b) which indicates increase of SRH recombination with acceptor concentration.

We attributed the effect of non-exponential PL decays to recombination through deep donor (DD) centers which ionization degree changes with concentration of excess electrons. Similar dependence of hole lifetime on excitation was observed in n-GaAs and was explained by hole capture to deep acceptor levels [21]. In InGaAs these centers may originate from vacancies in the lattice structure or may be associated with Zn–doping. The undoped materials exhibit n-type conductivity with supports the assumption of DD centers. In intentionally-n-type-doped materials with Fermi levels near the conduction band edge or above that these centers N are occupied with electrons and stay neutral, $N^0 = N - N^+ \approx N$. Here N^0 and N^+ are concentrations of neutral and ionized centers, respectively. In contrast, in p-doped InGaAs materials with Fermi levels near the valence band edge the DD centers are compensated by acceptors and remain positively charged in

equilibrium conditions because of practically complete ionization, $N^+ \approx N$. Under low excitation conditions the positively-charged centers capture non-equilibrium electrons with a high rate due to Coulomb attraction (Figure 10a). Thus, kinetics of electron lifetime in the conduction band under low injection conditions is controlled by the process of electron capture to the DD centers with cross-section σ_n that defines the minority carrier lifetime $\tau_{low\_inj} = (\sigma_n v_{th} N)^{-1}$, where v_{th} is the thermal velocity.

With increase of the excitation intensity the excess electron concentration increases and quasi-Fermi level for electrons approaches the energy level of the DD centers (Figure 10b) resulting in population of these centers with electrons (deionization of centers). When the DD centers are neutral, $N^0 \approx N$, the recombination rate is limited by cross-section of capture of holes to the centers, σ_p. The latter is significantly smaller than σ_n due to absence of Coulomb attraction, $\sigma_p << \sigma_n$, and, thus, for moderate excitations the SRH electron lifetime is larger $\tau_{high\_inj} = (\sigma_p v_{th} N)^{-1}$. In moderately doped materials under these excitations the overall electron lifetime is controlled by both SRH and radiative recombination processes. In order to separate their contributions temperature dependences of electron lifetime was measured under elevated excitations when the DD centers are saturated with electrons, $(\sigma_p/\sigma_n)\, N_A < \Delta n << N_A$ (see the linear fit in Figure 9). Both measured and calculated temperature dependences of electron lifetime are shown in Figure 11. The calculations included accounting for temperature dependences of the photon recycling coefficient and energy bandgap. The target doping values are shown in the Figure. Dependence of the photon recycling on doping was neglected since the latter was varied in a relatively narrow range. Dependence of the photon recycling in the 0.6 eV InGaAs DHs in a wide range of doping will be published elsewhere [[12]]. Both the experimental and theoretical electron lifetimes decrease with decrease of temperature as expected. The integrated PL intensity was found increasing with cooling due to relative increase of the contribution of radiative recombination term however at liquid nitrogen temperatures that increase saturated to a constant level. Thus, it was assumed that at the liquid nitrogen temperature electron lifetimes are completely controlled by radiative processes. The same assumption was made in analysis of temperature dependences of the PL intensity measured in similar 0.6 eV InGaAs structures in [[22]]. The fittings of calculations to the experimental data in Figure 11 were made with free carrier

concentration as a parameter. The adopted assumption would lead to determination of lower limits for non-radiative recombination terms.

One can see that experimental data for electron lifetime show slower temperature dependence compared to the corresponding radiative recombination terms and, in spite of saturation of DD recombination centers, non-radiative recombination processes contribute significantly at room temperature. One can note that the non-radiative recombination term increases with doping concentration. Temperature dependences of non-radiative terms were found to be weak which allowed for assumption of the SRH nature of those terms. Parameters β shown in Figure 11 were extracted from experimental data in the temperature range of T = 80…200 K for comparison with β = 1.23 obtained by calculations for the radiative term. One can see decrease of experimental value of β-parameter with doping indicating increase of the SRH recombination with concentration of Zinc. From the fittings shown in the Figure it was concluded that at room temperatures the non-radiative term increases approximately linearly with acceptor concentration. For given doping values and having all acceptors ionized, its lower limit at room temperature was approximated as $1/\tau_{NR} \approx 3.4 \cdot 10^{-11} \cdot N_A$, where N_A is Zinc concentration. For comparison, the fitting of radiative terms in Figure 11 resulted in $1/\tau_{Rad} = 4.0 \cdot 10^{-11} \cdot p$. Approximate proportionality of the non-radiative lifetime to the acceptor doping makes it ineffective in reduction of the TPV device dark current. The rapid degradation of electron lifetime under low injection was found progressing with doping. This effect sets some requirements on minimum excitation necessary to keep the deep-donor recombination centers saturated. Thus, decrease of p-type doping concentration is expected to improve the electron lifetime for lower excitations and the device open circuit voltage, respectively.

6. Conclusions

Minority carrier lifetime was measured in sets of Tellurium and Zinc doped DHs with 0.6 eV InGaAs active regions. Temperature dependences of minority carrier lifetime were analyzed from cryogenic to above-room temperatures in order to separate contributions of radiative and non-radiative recombination terms. The radiative terms were calculated based on the actual absorption edge spectrum. It was found that the materials show

slower than $T^{1.5}$ temperature dependences of radiative lifetime due to inconsistency of the absorption edge spectrum with the ideal square-root model. It was found that these dependences are different for electrons and holes and the difference increases with cooling. Temperature dependences of the photon recycling coefficient and energy bandgap were taken into account in the analysis.

It was concluded that in Te-doped InGaAs the radiative lifetime controls the hole lifetime at cryogenic temperatures while non-radiative processes dominate at room temperatures for free carrier concentrations about 10^{17} cm^{-3} and above. The nonradiative recombination was attributed to Auger process with room temperature coefficient C_n =3.2 x 10^{-28} cm^6/s due to square dependence on free carrier concentration. Comparison of the experimental data with estimation of C_n for the CHCC Auger process was performed. Assuming domination of the CHCC transitions, the activation energy of 40 meV was extracted from the experimental data. This value is smaller than the value predicted by calculations in the approximation of isotropic valence bands.

In Zn-doped materials rapid decrease of instantaneous electron lifetime with decrease of excitation was observed. This effect was explained by capture of excess electrons by ionized deep donor recombination centers. Temperature dependences of electron lifetime were measured under excitations corresponding to saturation of these centers with electrons. Essential contribution of SRH recombination to the electron recombination rate at room temperatures was observed. Increase of the SRH recombination in proportion to the acceptor doping makes the p-doping ineffective in reduction of the TPV device dark current. Improvement of the TPV device open circuit voltage with decrease of *Zn* concentration in the TPV absorber below p = 1x10^{17} cm^{-3} is expected due to relaxed requirements on saturation of deep donor recombination centers.

7. Acknowledgements

The authors appreciate the valuable discussions and encouragement from Gregory Belenky and Serge Luryi as well as assistance of Sergei Anikeev and Gu Ning with measurements.

8. Appendix

Let us continue the analysis in paragraph 3 with approximation for the absorption edge spectrum in the form $A\sqrt{h\nu - \varepsilon_g}/h\nu$. Typically, the absorption spectrum is measured in undoped materials so that one can neglect the band filling effects due to f_c, $f_v << 1$ and constant A is obtained by fitting of the model dependence to the experimental spectrum.

$$dq_{sp} = \frac{\alpha(h\nu)}{1 - f_v^h - f_c^e}\frac{c}{N} f_c^e f_v^h \rho d\nu \approx A\frac{\sqrt{h\nu - \varepsilon_g}}{h\nu}\frac{c}{N} f_c^e f_v^h \rho d\nu \qquad (12)$$

Use of carrier distribution functions with quasi-Fermi levels F_e and F_h results in

$$dq_{sp} = A\frac{8\pi N^2}{h^3 c^2}\frac{h\nu\sqrt{h\nu - \varepsilon_g}}{\left(\exp\left(\frac{\varepsilon_c(\nu) - F_e}{k_B T}\right)+1\right)\left(\exp\left(\frac{\varepsilon_v(\nu) - F_h}{k_B T}\right)+1\right)} d(h\nu) \qquad (13)$$

$$Q_{sp} = A\frac{8\pi N^2}{h^3 c^2}\int_{\Delta\varepsilon=0}^{\infty}\frac{\left(\varepsilon_g + \Delta\varepsilon\right)\sqrt{\Delta\varepsilon}}{\left(\exp\left(\frac{\Delta\varepsilon\, m_{cv}/m_c - F_e}{k_B T}\right)+1\right)\left(\exp\left(\frac{\Delta\varepsilon\, m_{cv}/m_v - F_h}{k_B T}\right)+1\right)} d(\Delta\varepsilon) \qquad (14)$$

We performed simulation of temperature dependence of minority carrier lifetime for electrons and hole using the square-root approximation for the absorption edge spectrum. The results are shown in Figure A1. Once can see that asymptotic $T^{1.5}$ is valid for both weakly-degenerate (Figure A1a) and non-degenerate (Figure A1b) carrier statistics within the range of temperatures and concentrations presenting practical interest for TPV device technology. The deviations from β=1.5 were observed for highly-degenerate cases realized in extremely-low temperature range where $k_B T << F_e$. F_h. With decrease of temperature these deviations were observed earlier for n-type material with smaller density of states compared to p-type one. The values of β-parameter for T^β were determined in the temperature range of T = 80..200 K for comparison with the calculated and experimental data presented in the paper above.

For illustrative purposes we validated analytically the asymptotics for temperature dependences of minority carrier lifetime for non-degenerate and degenerate carrier statistics. For simplicity only temperature-dependent terms were carried out.

1. Non-degenerate approximation, sub-index notations correspond to electron lifetime $p \propto T^{3/2} \cdot \exp(F_h / k_B T)$, using substitution $x = \Delta\varepsilon/k_B T$ one can obtain

$$Q_{sp} \propto \exp\left(\frac{F_e + F_h}{k_B T}\right)(k_B T)^{5/2} \int_{\varepsilon=0}^{\infty} \left(\frac{\varepsilon_g}{k_B T} + \varepsilon\right)\sqrt{\varepsilon}\exp(-\varepsilon)d\varepsilon \propto \exp\left(\frac{F_e + F_h}{k_B T}\right)(k_B T)^{3/2}\varepsilon_g \quad (15)$$

Since the integral value is defined in the range of energy ε of several $k_B T$ and in the practical range of temperatures $\varepsilon << \varepsilon_g/k_B T$, one can neglect the second term in the integral expression which makes the integral value independent on temperature. Thus, for electron lifetime one can use asymptotic as follows

$$\tau = \frac{\Delta n}{Q_{sp}} \propto \frac{T^{3/2}\exp(F_e / k_B T)}{\exp(F_e + F_h / k_B T)T^{3/2}\varepsilon_g} = \frac{1}{\varepsilon_g \exp(F_h / k_B T)} = \frac{T^{3/2}}{\varepsilon_g p} \quad (16)$$

2. Degenerate approximation, sub-index notations correspond to hole lifetime, $n \propto (F_e)^{3/2}$, in this case there is no exponential terms and integration is performed up to Fermi energy F_e

$$Q_{sp} = \exp\left(\frac{F_h}{k_B T}\right)(k_B T)^{3/2}\varepsilon_g \int_{\varepsilon=0}^{F_e} \sqrt{\varepsilon}d\varepsilon = \exp\left(\frac{F_h}{k_B T}\right)(k_B T)^{3/2}\varepsilon_g \frac{2}{3}F_e^{3/2} \quad (17)$$

$$\tau = \frac{\Delta p}{Q_{sp}} \propto \frac{T^{3/2}\exp(F_h / k_B T)}{\exp(F_h / k_B T)T^{3/2}\varepsilon_g F_e^{3/2}} = \frac{1}{\varepsilon_g F_e^{3/2}} \quad (18)$$

Validity of $\beta = 1.5$ dependence in a wide range of temperatures including intermediate weakly-degenerate statistic is explained by similarity of the structure of integral for Q_{sp} in denominator and the Fermi integral in numerator of the expression for carrier lifetime.

Neglecting term ε in comparison to E_g/k_BT in transition from (12) to (13) makes the integral for Q_{sp} identical to the Fermi integral. Thus, mutual cancellation of both integral terms leaves only the temperature dependence of density of states for non-equilibrium carriers which are non-degenerate by default.

Figures and figure captions

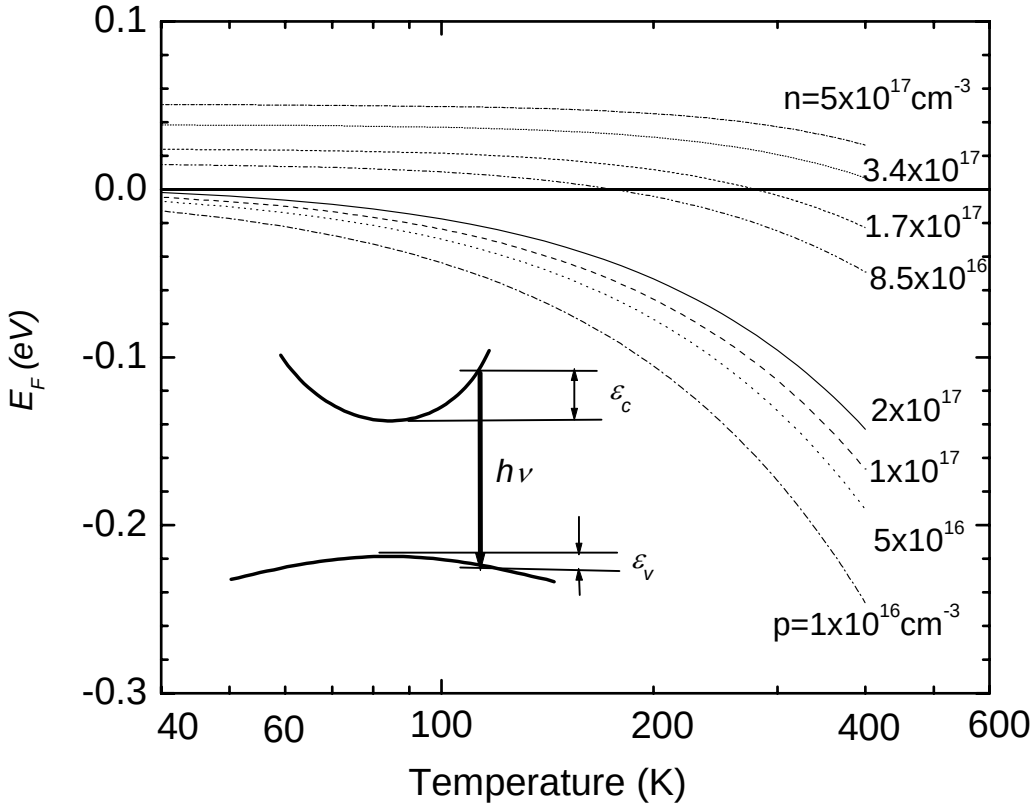

Figure 1. Temperature dependences of quasi-Fermi levels for electron and hole distributions in 0.6 eV InGaAs. Schematic of the band diagram with electron and hole energies ε_c and ε_v corresponding to direct optical transitions with energy $h\nu$ is shown in the inset. The quasi-Fermi levels are shown with respect to the minimum and maximum of the conduction and valence bands, respectively.

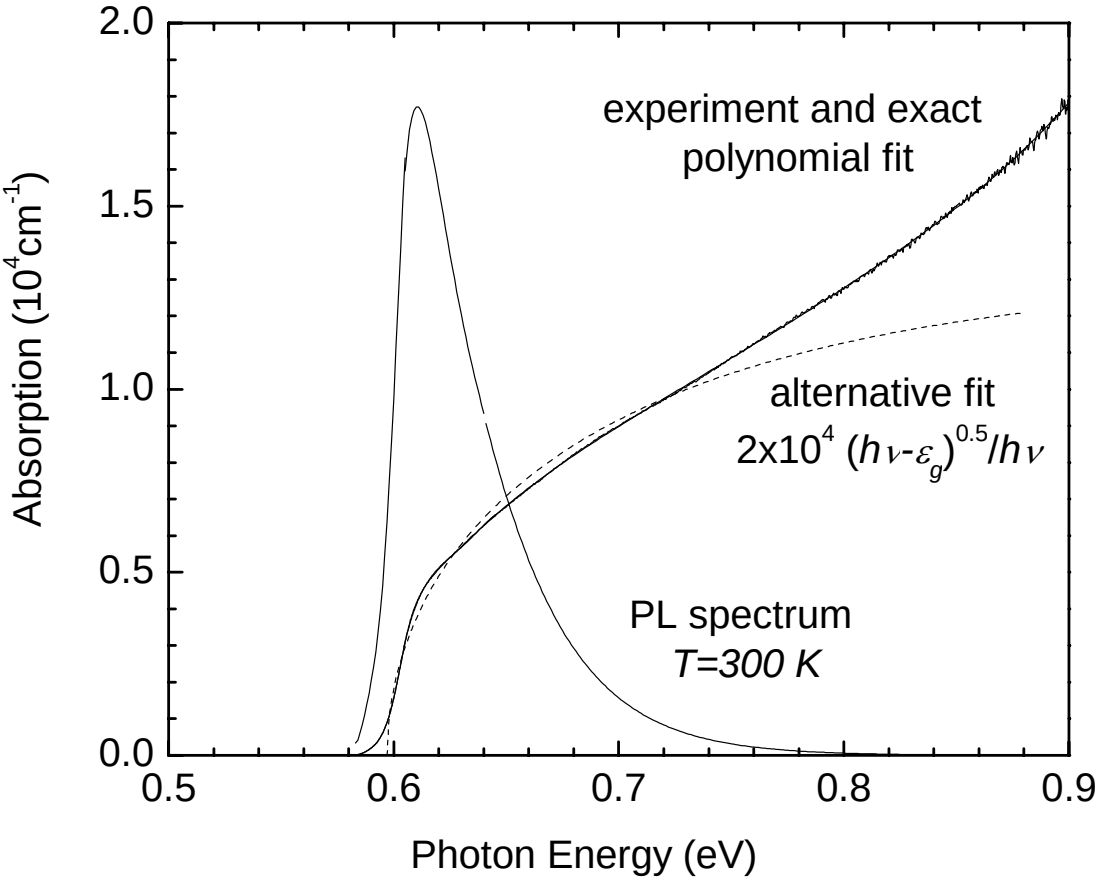

Figure 2. Experimental absorption spectrum, its exact polynomial fit and room-temperature spontaneous emission spectrum calculated from that dependence. One can see that the alternative modeling with expression $A\sqrt{h\nu-\varepsilon g}/h\nu$ fails to provide an adequate fit.

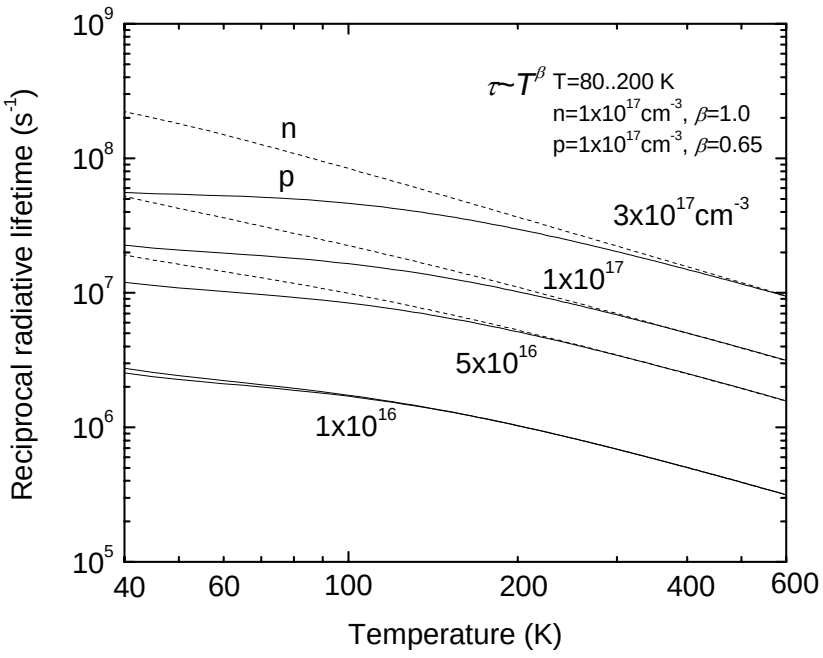

Figure 3. Electron (solid lines) and holes (dashed lines) minority carrier lifetime in p-type and n-type materials, respectively, calculated by integration of the experimental absorption spectrum. The β parameter shown was determined comparison with experiment in the temperature range of T = 80- 200 K for materials with p= 1 x 10^{17} cm^{-3}.

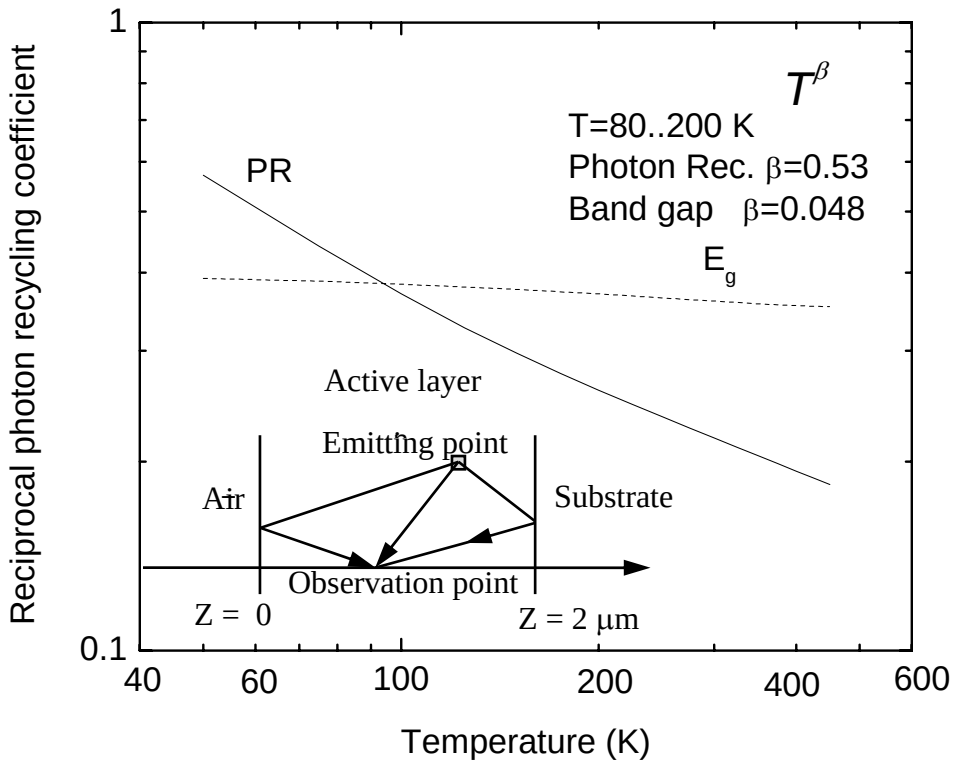

Figure 4. Temperature dependences of the photon recycling coefficient and energy band gap. The inset shows the reflected components taken into account in calculation of the photon recycling.

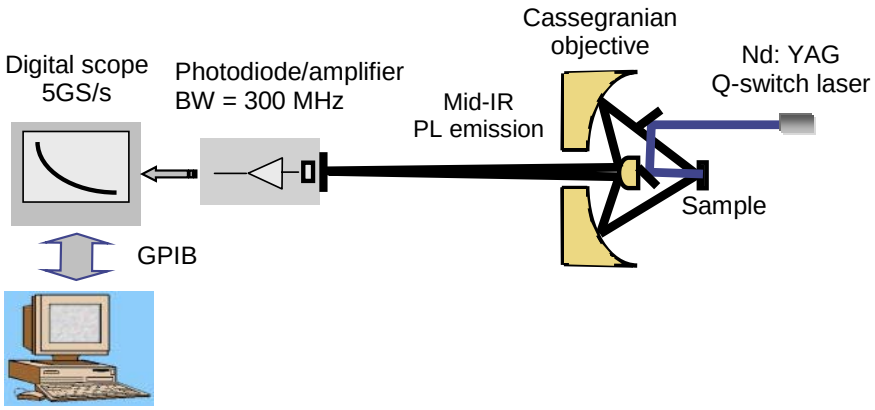

Figure 5. Schematic diagram of the experimental setup. The excess carriers were excited at 532 nm or 1,064 nm by Q-switched Nd:YAG laser with a pulse with of 0.5 ns and repetition rate of 6 kHz. The photoluminescence was collected with reflective optics and focused on a small-area photodiode with a sub-ns decay time constant. The PL decays were recorded with a digital scope with a sampling rate of 5 GS/s.

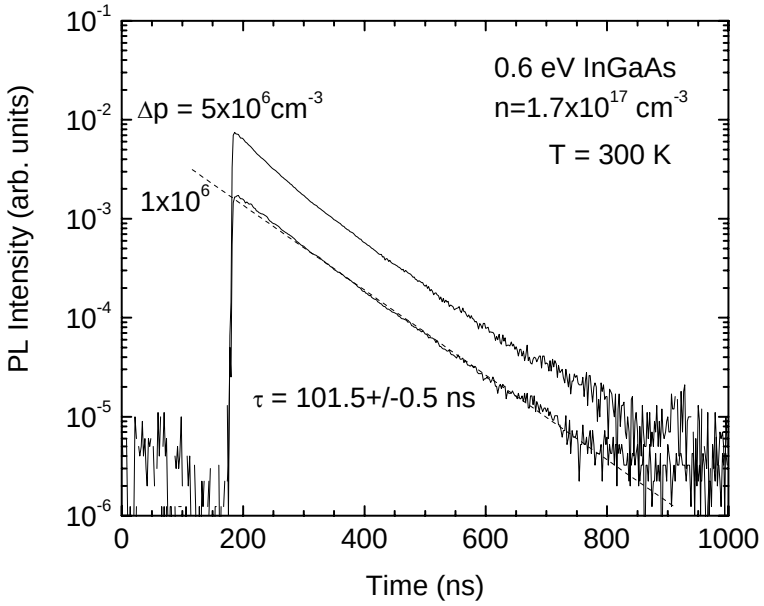

Figure 6. Typical PL decays obtained in the double heterostructures with Te-doped active layers. Excess carrier concentrations shown correspond to the maxima of PL decays. The time constant was obtained by an exponential fit over two-orders of magnitude of PL intensity.

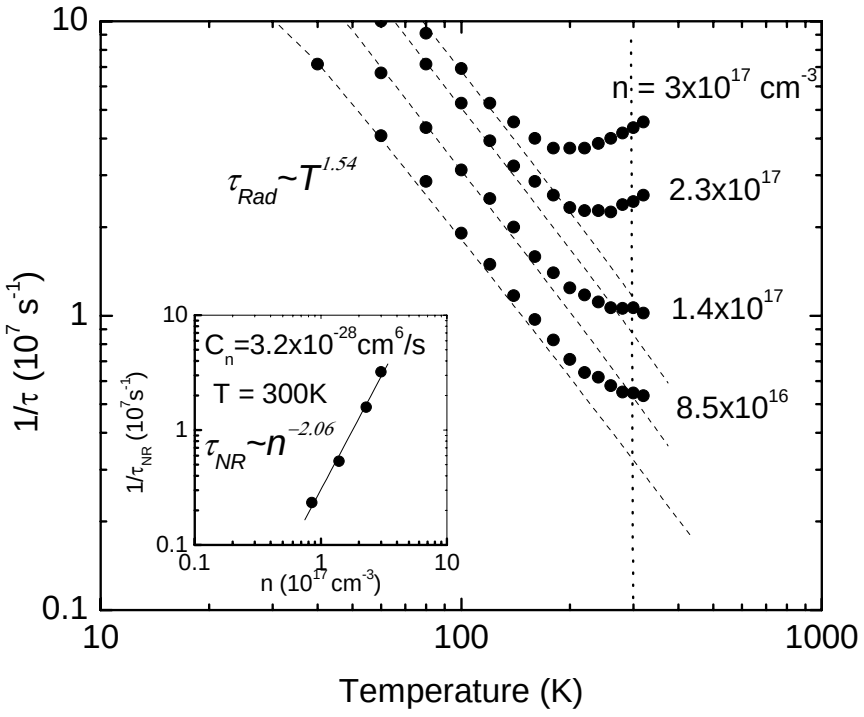

Figure 7. Temperature dependences of hole lifetime in double heterostructures with 0.6 eV InGaAs active layers doped with different Tellurium doping levels. Dashed lines show fitting obtained in accordance with the analysis in paragraph 3. The non-radiative part of the lifetime constants versus free carrier concentration obtained by fitting of the radiative term are shown in the inset.

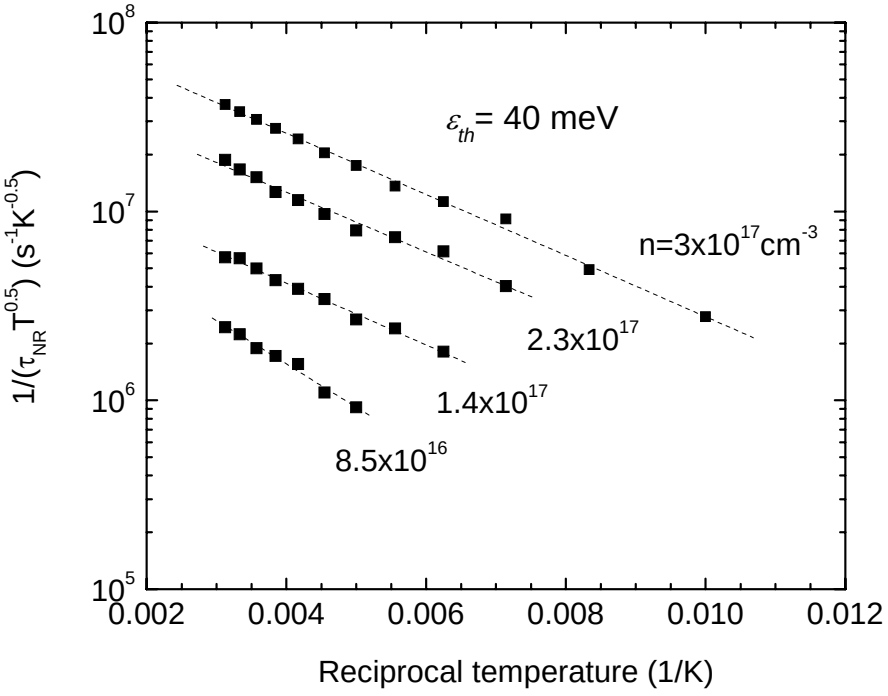

Figure 8. Activation energy for Auger process extracted from temperature dependences of non-radiative recombination in n-type 0.6 eV InGaAs heterostructures.

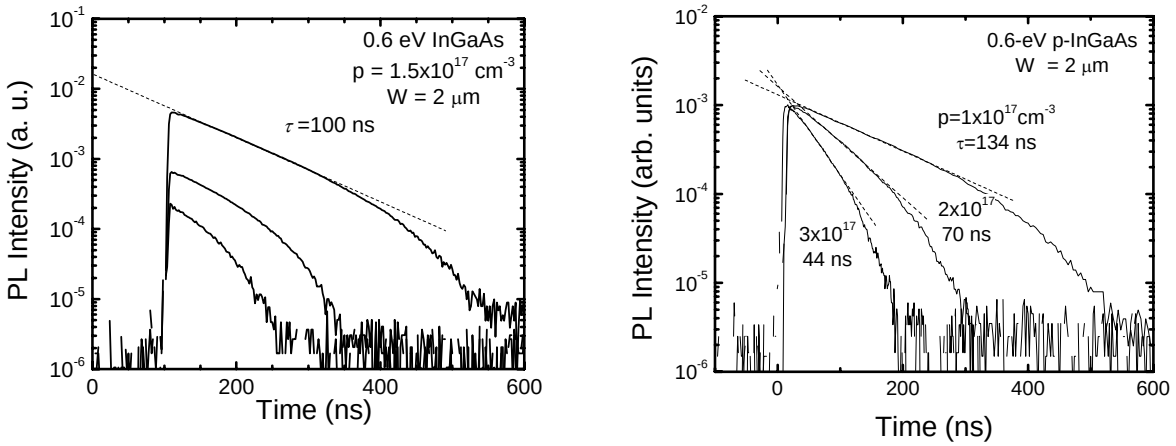

(a) (b)

Figure 9. Typical PL decays measured in p-type DHs at different excitation levels (a) and for different acceptor concentrations (b). Peaks of PL decays correspond to low injection conditions with initial excess carrier concentrations below background free carrier concentrations. Decrease of excess carrier concentration leads to rapid decrease of lifetime attributed to capture on ionized deep donor (DD) recombination centers. Dashed line fit corresponds to excitation when the DD centers are saturated with excess electrons. Note rapid decrease of instantaneous time constants at tails of PL decays which progresses with acceptor doping.

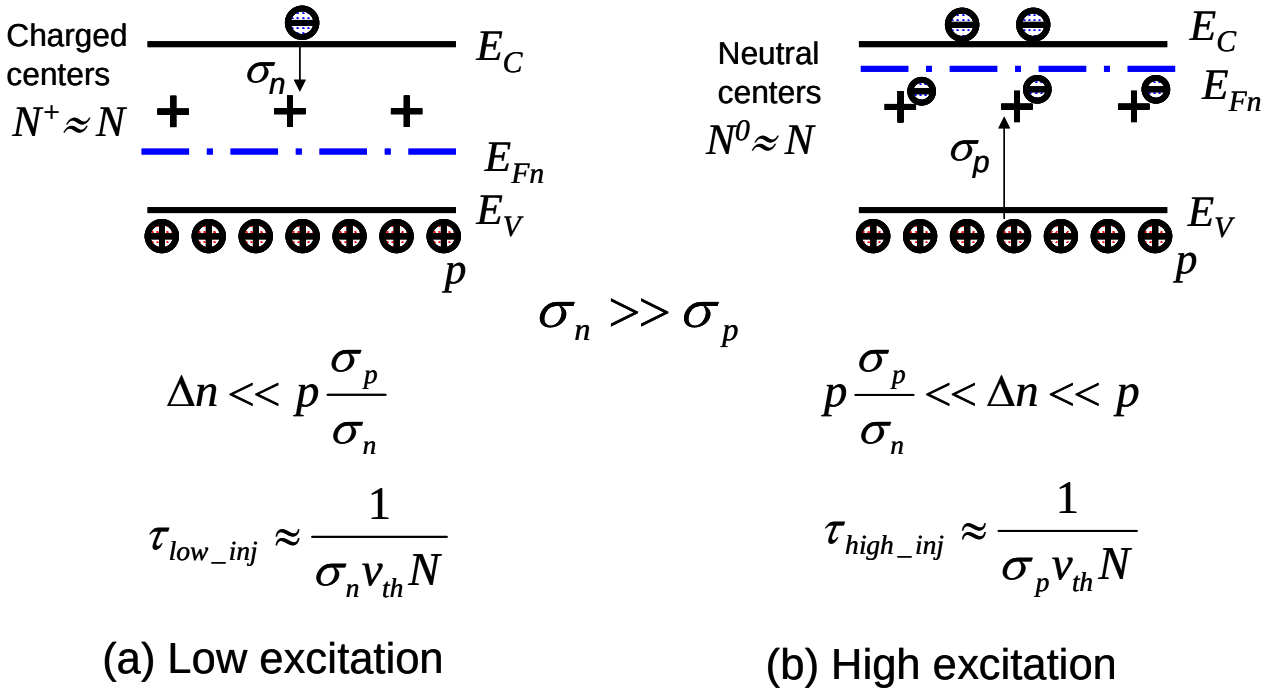

Figure 10. Schematic of energy band diagram with deep donor (DD) recombination centers: (a) low injection, the DD centers are ionized (positively charged) and are able to capture non-equilibrium electrons, the electron lifetime is controlled by capture cross-section of electrons to the center; (b) high injection, the DD centers are occupied with electrons, the electron lifetime is limited by capture cross-section of majority holes to the neutral DD centers.

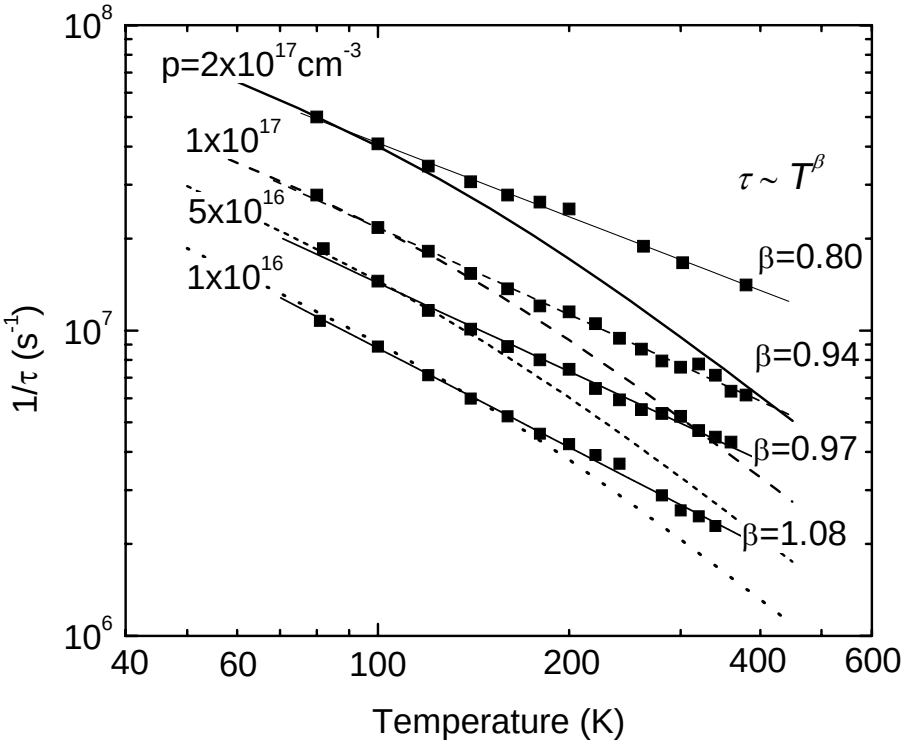

Figure 11. Temperature dependence of electron lifetime in p-doped 0.6 eV InGaAs measured under low injection condition with saturation of deep donor recombination centers ($p\sigma_p/\sigma_n << \Delta n << p$). The points show experimental data, solid and dashed lines represent fits with radiative recombination terms obtained in accordance with analysis in paragraph 3. The β-parameter in T^β was extracted for experimental data in the temperature range of T = 80...200 K for comparison with results of calculation.

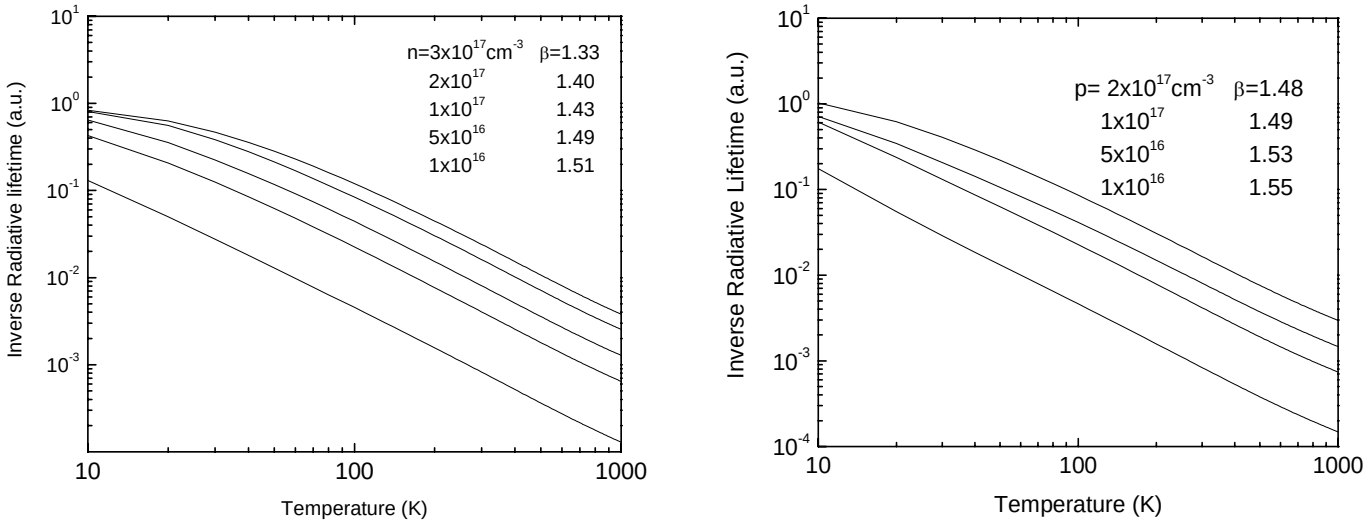

(a) (b)

Figure A1. Temperature dependences of minority carrier lifetime in a generic material with square-root approximation for the absorption edge spectrum (a) for holes in n-type material and (b) for electrons in p-type materials. Once can see that asymptotic $T^{1.5}$ for temperature dependence of minority carrier lifetime is valid for both degenerate (a) and non-degenerate (b) carrier statistics. The values of β-parameter for T^{β} were determined in the temperature range of T = 80..200 K for comparison with other data discussed.

References

[1] D. Wilt et. al., "InGaAs PV device development for TPV power systems", 1st NREL Thermophotovoltaic Generation of Electricity Conference, *AIP Conf. Proc*., **321**, 210-220 (1994)

[2] M. W. Wanlass, et. al., "GaInAs Thermophtovoltaic Converters", *Sol. Energy Mater. Sol. Cells*, **41/42**, 405 (1996)

[3] R. K. Ahrenkiel, S. W. Johnston, J. D. Webb, L. M. Gedvilas, J. J. Carapella, and M. W. Wanlass, "Recombination lifetimes in undoped, low-band gap $InAs_yP_{1-y}/In_xGa_{1-x}As$ double heterostructures grown on InP substrates", *Appl. Phys. Lett.,* **78**, 8, 1092-1094 (2001)

[4] D. Wilt, R .Wehrer , M. Palmisiano , M. Wanlass , C. Murray , "Monolithic interconnected modules (MIMs) for thermophotovoltaic energy conversion", *Semic.Sci. Tecnol.*, **18** (5), S209-S215 (2003)

[5] B. Wernsman, RR Siergiej, S.D. Link, R.G. Mahorter, M.N. Palmisiano, R.J. Wehrer, R.W. Schultz, G.P. Schmuck , R.L. Messham , S. Murray, C.S. Murray, F. Newman, D. Taylor, D.M. DePoy, T. Rahmlow, "Greater than 20% radiant heat conversion efficiency of a thermophotovoltaic radiator/module system using reflective spectral control", *IEEE Trans. on Electron Devices*, 51(3), 512-515 (2004)

[6] T. H. Gfrorer, L. P. Priestley, M. F. Fairley, M. W. Wanlass, "Temperature dependence of non-radiative recombination in low-bandgap InGaAs/InAsP double hetrostructures grown on InP substrates", *J. of Appl.Phys.*, **94**(3), 1738-1743 (2003)

[7] R. K. Ahrenkiel, R. Ellingson, S. Johnston, J. Webb, J. Carapella, and M. Wanlass, "Recombination Lifetime of $In_xGa_{1-x}As$ Alloys Used in Thermophotovoltaic Converters", *AIP Conf. Proc*., **460**, p. 282, (1999)

[8] P. T. Landsberg, "Recombination in semiconductors", Cambridge University Press, 1991

[9] N. G. Nilsson, *Phys. Sta. Solidi (a)*, **19**, K75 (1973).

10 P. Asbeck, "Self-absorption effects on radiative lifetime in GaAs- GaAlAs double heterostrtuctures", *J. Appl. Phys.*, **48**, 820-822 (1977)

11 R. K. Ahrenkiel, B. M. Keyes, G. B. Lush, M. R. Melloch, M. S. Lundstrom, and H. F. MacMillan, "Minority-Carrier lifetime and Photon Recycling in n-GaAs", *J. Vac. Sci. Technol*., **A 10**, 990 (1992)

[12] T. Kuriyama,T. Kamiya, H. Yanai, "Effect of photon recycling on diffusion length and internal quantum efficiency in AlxGa1-xAs-GaAs heterostructures", *Japan. J. Appl .Phys.*, **16**(3) 465-477 (1977)

[13] D. Donetsky, F. Newman, M. Dasheill, "Carrier recombination processes in epitaxial materials for thermophotovoltaic devices" (to be submitted to *Semicond. Sci. Technol*.)

[14] S. L. Murray, F. D. Newman, C. S. Murray, D. M. Wilt, M. W. Wanlass, P. Ahrenkiel, R. Messham and R. R. Siergiej, "MOCVD growth of lattice-matched and mismatched InGaAs materials for thermophotovoltaic energy conversion", *Semicond. Sci. Technol.* **18,** S202-S208 (2003)

[15] F.D. Newman, M.A. Stan, S.L. Murray, et al., "Tellurium surfactant effects in the growth of lattice mismatched InAsxP1-x, by metal organic vapor-phase epitaxy", *J. of Crystal Growth*, **272** (1-4): 650-657 (2004)

[16]D. Donetsky, S. Anikeev, G. Belenky, et al., "Reduction of interfacial recombination in GaInAsSb/GaSb double heterostructures", *Appl. Phys. Lett.*, **81** (25): 4769-4771 (2002)

[17] W. K. Metzger, M. W. Wanlass, R. J. Ellingson, R. K. Ahrenkiel, and J. J. Carapella, "Auger recombination in low-band-gap n-type InGaAs", *Appl. Phys. Lett.*, **79** (20), 3272-3274 (2001)

[18] S. Hausser , G. Fuchs , A. Hangleiter , K. Streubel , W.T. Tsang , "Auger recombination in bulk and quantum-well InGaAs", *Appl. Phys. Lett.*, **56** (10): 913-915 (1990)

[19] V. N. Abakumov, V.I. Perel, Y.N. Yassievich, "Carrier recombination processes in semiconductors", 1991

[20] P. Rees, P. Blood, M. J. H. Vanhommerig, G. J. Davies, and P. J. Skevington, *J.Appl. Phys.*, **78**, 1804 (1995)

[21] R. K. Ahrenkiel, B. M. Keyes, D. J. Dunlavy, "Intensity-dependent minority-carrier lifetime in III-V semiconductors due to saturation of recombination centers", *J. Appl. Phys.*, **70**, 1, 227-231 (1991)

[22]T. H. Gfroerer, C. E .Gillespie, J. P. Campbell, and M. W. Wanlass, **"**Deep donor-acceptor pair recombination in InGaAs-based heterostructures grown on InP substrates", *J. Appl. Phys*., **98**, 093708 (2005)